

Supplementary Information

Sustainable ammonia synthesis through electrochemical dinitrogen activation using $\text{Ag}_2\text{VO}_2\text{PO}_4$ catalyst

Divyani Gupta, Alankar Kafle and Tharamani C. Nagaiah*

Materials and reagents used

The catalyst was synthesized using the precursors silver nitrate (AgNO_3 ; $\geq 99.8\%$) from Chemlab, ammonium metavanadate (NH_4VO_3) from Loba chemie, phosphoric acid (H_3PO_4) from Merck which are of analytical grade and have been used as such without further purification. Ammonium chloride, salicylic acid, sodium nitroprusside, para-dimethylaminobenzaldehyde, sodium nitrate, sodium nitrite, sulphanilamide, N-(1-Naphthyl) ethylenediamine dihydrochloride, mercuric (II) iodide, sodium potassium tartrate, hydrazine monohydrate, sodium hypochlorite solution and hydrogen peroxide solution were purchased from Loba chemie and used for quantification purpose. $^{15}\text{NH}_4\text{Cl}$ (99%) was bought from Cambridge isotope laboratories. All solutions were prepared using deionized water obtained from Millipore system (15 M Ω). Potassium hydroxide, hydrochloric acid, and ethanol ($\text{C}_2\text{H}_5\text{OH}$; 99 %) were purchased from Loba chemie and Merck and were used as such without further purification for solvent preparation in this work and Nafion N117 membrane was bought from DuPont. High purity $^{14}\text{N}_2$ (99.999%), $^{15}\text{N}_2$ (99%) and Ar gas (99.999%) cylinders were purchased from Sigma. The deionized water was obtained from Millipore system (>12 M Ω cm $^{-1}$).

Product/contaminants quantification methods

NH_3 & N_2H_4 quantification: The amount of ammonia was quantified by means of UV-Visible spectrophotometric method by Indophenol blue method and Nessler's reagent test as given in previous reports. The amount of hydrazine was also determined using UV-Vis. spectroscopy via Watt-Chrisp method.¹

NO_3^- & NO_2^- quantification: Any source of contamination in electrolyte solutions such as NO_3^- / NO_2^- was identified by means of UV-Vis. spectroscopic technique after following previously reported methods.¹

N_2O quantification: Quantification of N_2O in gas feed streams was performed by using gas-chromatography-mass spectroscopy (GC-MS) technique in selected ion monitoring (SIM) mode by using previously reported literature.²

Isotope labelling experiments

The NRR isotope labelling experiments were performed for $\text{Ag}_2\text{VO}_2\text{PO}_4$ (s) catalyst at -0.2 V by taking $^{15}\text{N}_2$ (Sigma-Aldrich 99 atom% ^{15}N) as the additional feeding gas than Ar and $^{14}\text{N}_2$. Prior to NRR measurements the gases were passed through the cleansing/scrubbing solution containing alkaline KMnO_4 in one tube followed by dilute H_2SO_4 solution in another tube where in a fixed amount of gas (250 mL gas) was supplied for the electrolysis.

^1H nuclear magnetic resonance measurements (^1H NMR) with water suppression method involved the application of a single pulse sequence during the relaxation delay of 1 s with a total number of 8000 transient scans and an acquisition time of 2.18 s for measurement of signal corresponding to $^{14}\text{NH}_4^+ / ^{15}\text{NH}_4^+$. DMSO- d_6 was added as an internal standard to achieve sufficient lock signal and 0.125 mL of maleic acid was added to the collected electrolyte sample for quantification purpose. Calibration curves were plotted standard $^{14}\text{NH}_4\text{Cl}$ and $^{15}\text{NH}_4\text{Cl}$ solutions (1-3 ppm) with reference to maleic acid by performing a total of 1024 scans.

Secondly, the liquid chromatography-mass spectroscopy (LC-MS) technique was utilised by following the reported procedure.^{3, 4}

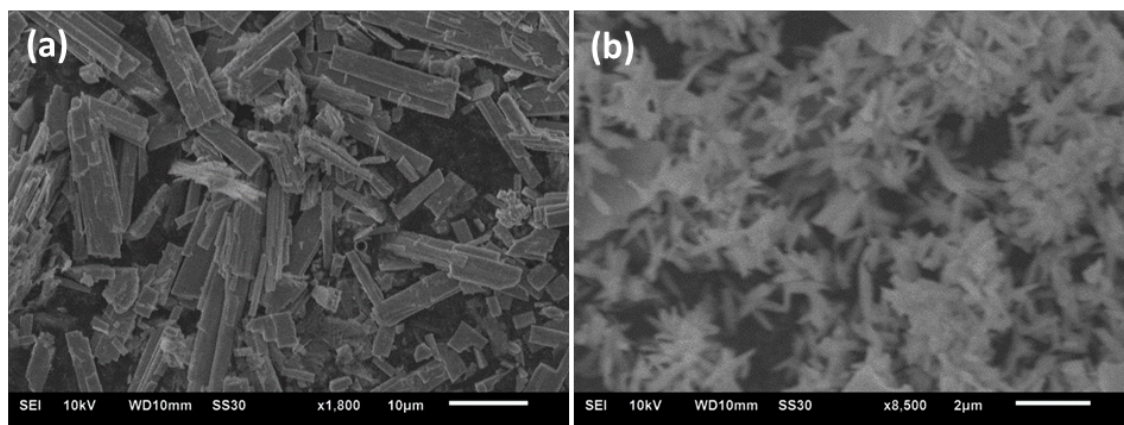


Fig. S1 SEM images of (a) $\text{Ag}_2\text{VO}_2\text{PO}_4$ (h) catalyst and (b) $\text{Ag}_2\text{VO}_2\text{PO}_4$ (s) catalyst.

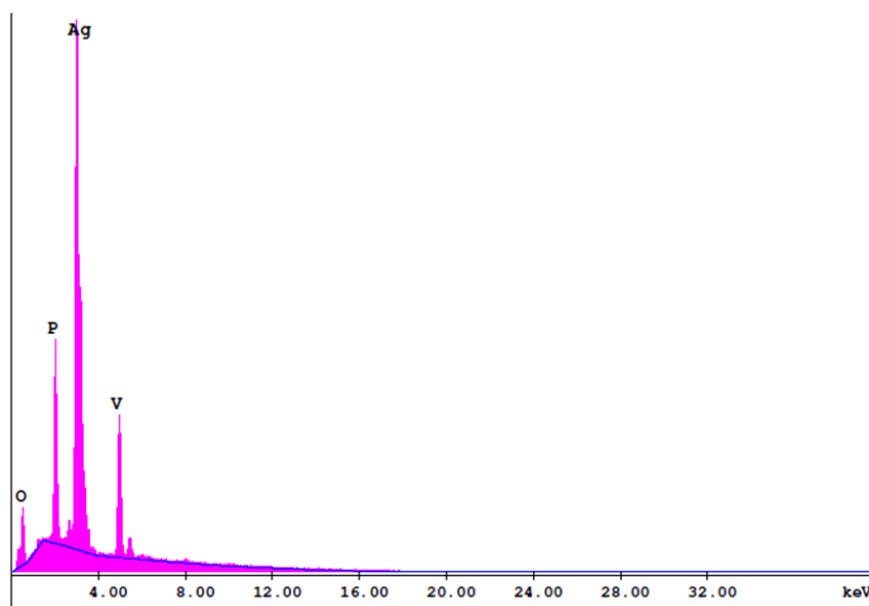


Fig. S2 EDS spectrum showing presence of Ag, V, P and O elements in $\text{Ag}_2\text{VO}_2\text{PO}_4$ (s) catalyst.

Table S1. Elemental compositional analysis from EDS spectrum of $\text{Ag}_2\text{VO}_2\text{PO}_4$ (s) catalyst		
Element	Wt %	At %
O K	13.75	42.93
P K	8.64	13.93
Ag L	63.74	29.53
V K	13.88	13.61
Total	100.00	100.00

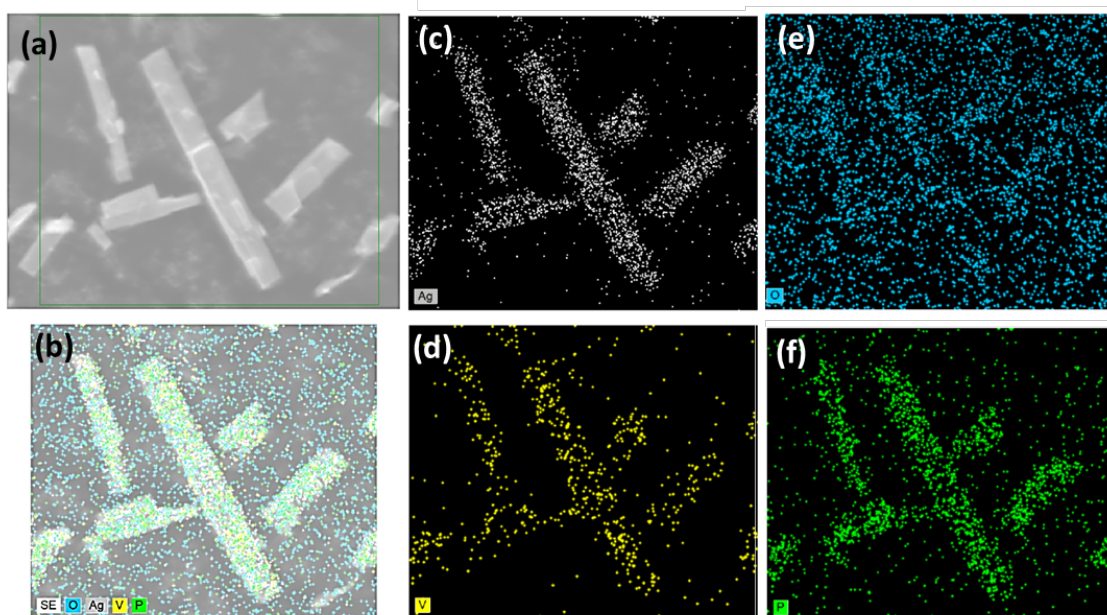


Fig. S3 EDS dot mapping profiles for individual elements of $\text{Ag}_2\text{VO}_2\text{PO}_4$ (h) catalyst over the scanned area.

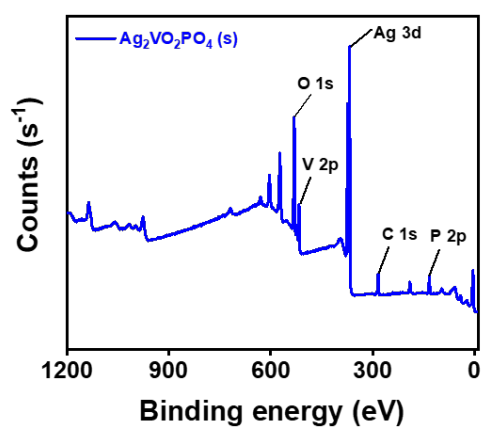


Fig. S4 XPS survey spectrum for $\text{Ag}_2\text{VO}_2\text{PO}_4$ (s) catalyst.

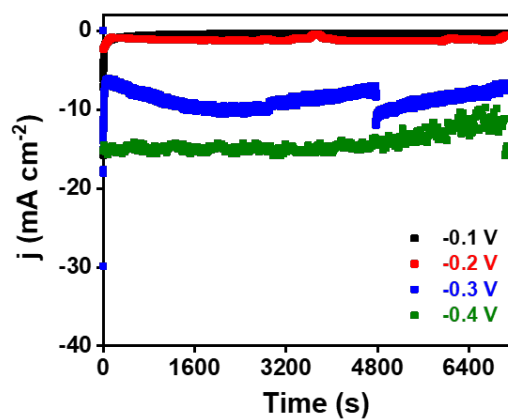


Fig. S5 Chronoamperometric curves obtained after applying external potentials between -0.1 to -0.4 V vs. RHE for 2 h during NRR by $\text{Ag}_2\text{VO}_2\text{PO}_4$ (s) catalyst.

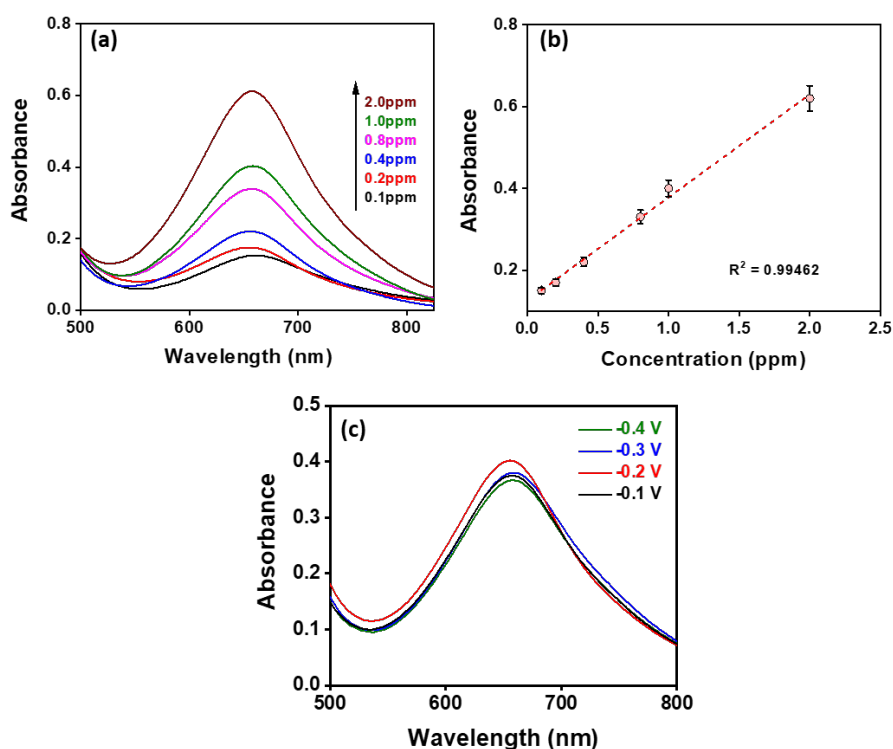


Fig. S6 (a) Absorbance vs. wavelength plots for standard NH_4^+ solutions obtained after Indophenol blue test and (b) corresponding calibration curve. (c) UV-Vis. curve for electrolyte samples collected after quantification by Indophenol blue method upon NRR by $\text{Ag}_2\text{VO}_2\text{PO}_4$ (s) catalyst.

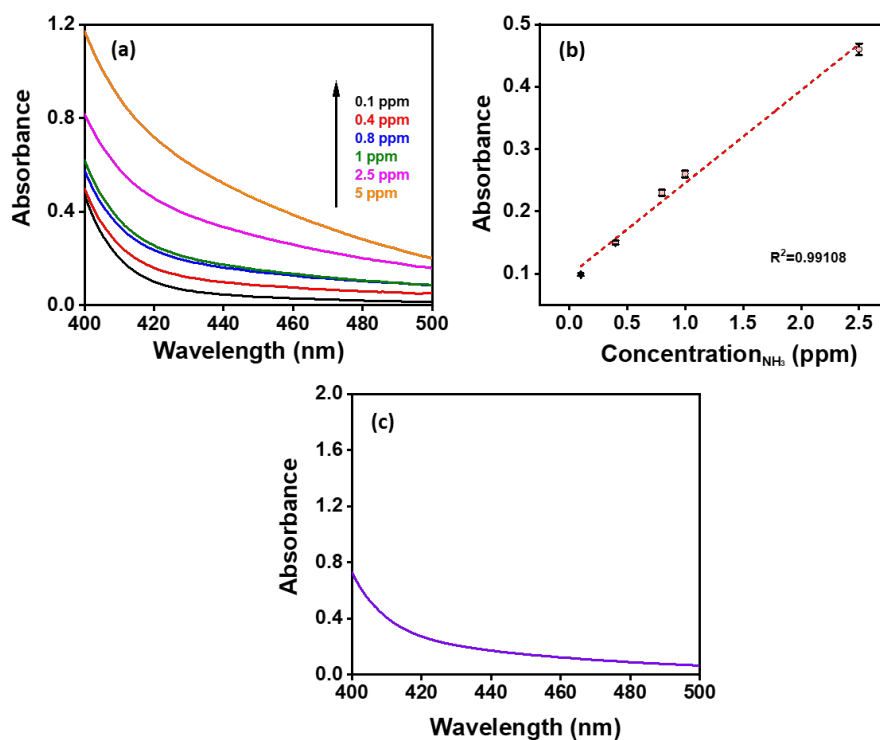


Fig. S7 (a) Absorbance vs. wavelength plots for standard NH_4^+ solutions obtained after Nessler's reagent test and (b) corresponding calibration curve. (c) UV-Vis. curve for electrolyte sample collected after quantification by Nessler's test upon NRR at -0.2 V by $\text{Ag}_2\text{VO}_2\text{PO}_4$ (s) catalyst.

Table S6A. Comparison of NH ₃ yield rates obtained after 2 h of e-NRR by Ag ₃ PO ₄ (2 h) at 0 V (vs. RHE).		
S.No.	NH ₃ detection method	NH ₃ yield rate (mg h ⁻¹ mg _{cat.} ⁻¹)
1.	Indophenol Blue	1.48
2.	Nessler's reagent	1.49

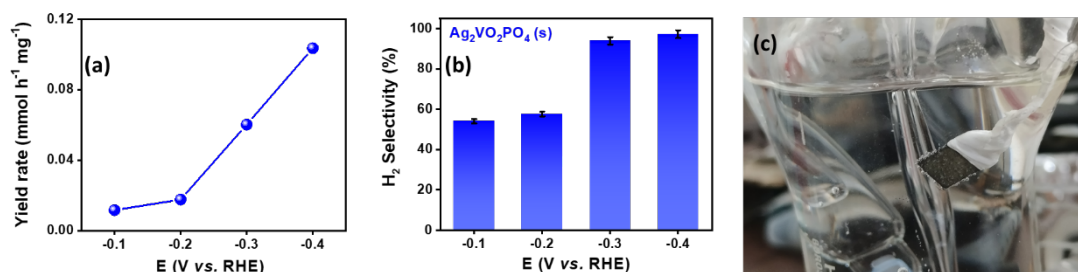


Fig. S8A (a) H₂ evolution yield rate and (b) H₂ selectivity (%) at different potentials calculated by GC. (c) Image showing the bubbles formation at electrode due to H₂ evolution in competition with NRR at -0.4 V.

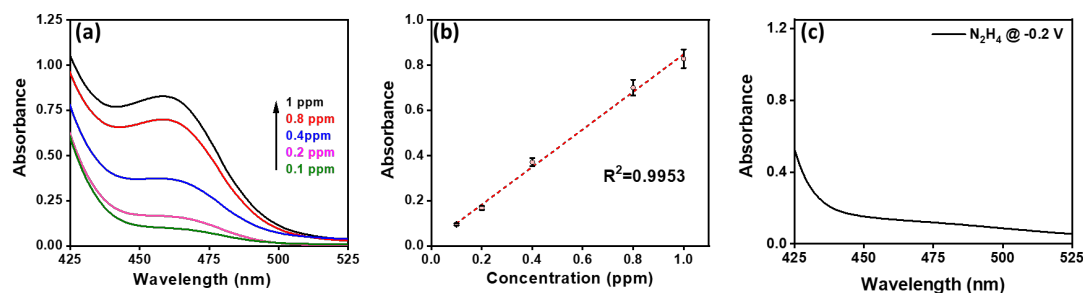


Fig. S8B (a) UV-Vis. absorbance curves for standard N₂H₄ solutions of different concentrations obtained after Watt-Chrisp quantification and (b) corresponding calibration curve extracted from the same. (c) UV-Vis. absorbance curve for electrolyte sample collected after NRR at -0.2 V for N₂H₄ detection.

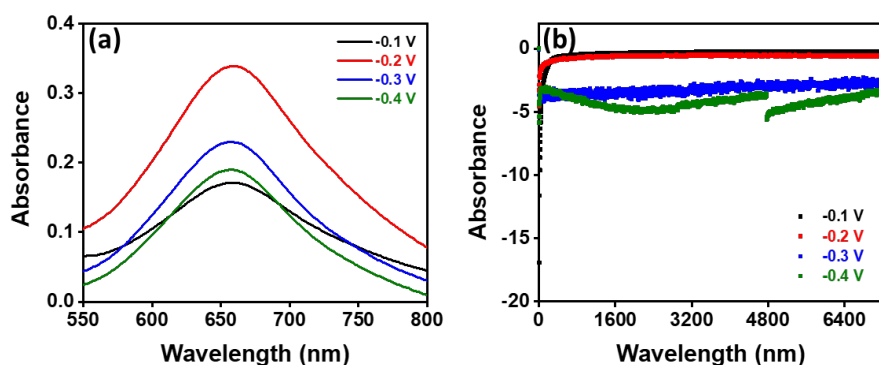


Fig. S9 (a) Absorbance vs. wavelength curves for electrolyte solutions collected after Indophenol blue quantification of samples obtained after NRR at different potentials by Ag₂VO₂PO₄ (h) catalyst and (b) chronoamperometric curves for NRR by Ag₂VO₂PO₄ (h).

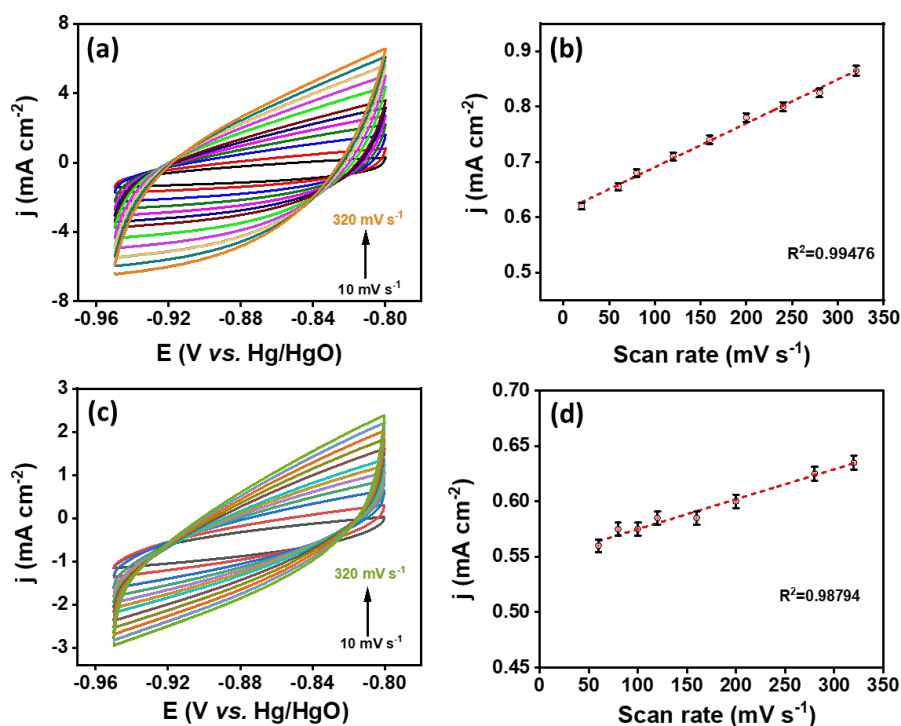


Fig. S10 (a, c) Cyclic voltammograms for $\text{Ag}_2\text{VO}_2\text{PO}_4$ (s), $\text{Ag}_2\text{VO}_2\text{PO}_4$ (h) catalyst at different scan rates and (b, d) corresponding current density vs. scan rate plots extracted from the CVs respectively.

Table S3A. Electrochemical surface area (ECSA) determination from Fig. S10. for different catalysts.			
S.No.	Electrocatalyst	C_{dl}^* (mF)	ECSA (cm^2)
1.	$\text{Ag}_2\text{VO}_2\text{PO}_4$ (s)	7.94	19.85
2.	$\text{Ag}_2\text{VO}_2\text{PO}_4$ (h)	2.698	6.745

Table S3B. Electrochemical Impedance analysis extracted from Fig. 3e.				
S. No.	Electrocatalyst	R_s (Ω)	R_p (Ω)	R_{ct} (Ω)
1.	$\text{Ag}_2\text{VO}_2\text{PO}_4$ (s)	24.53	233.83	209.30
2.	$\text{Ag}_2\text{VO}_2\text{PO}_4$ (h)	20.06	271.95	251.89

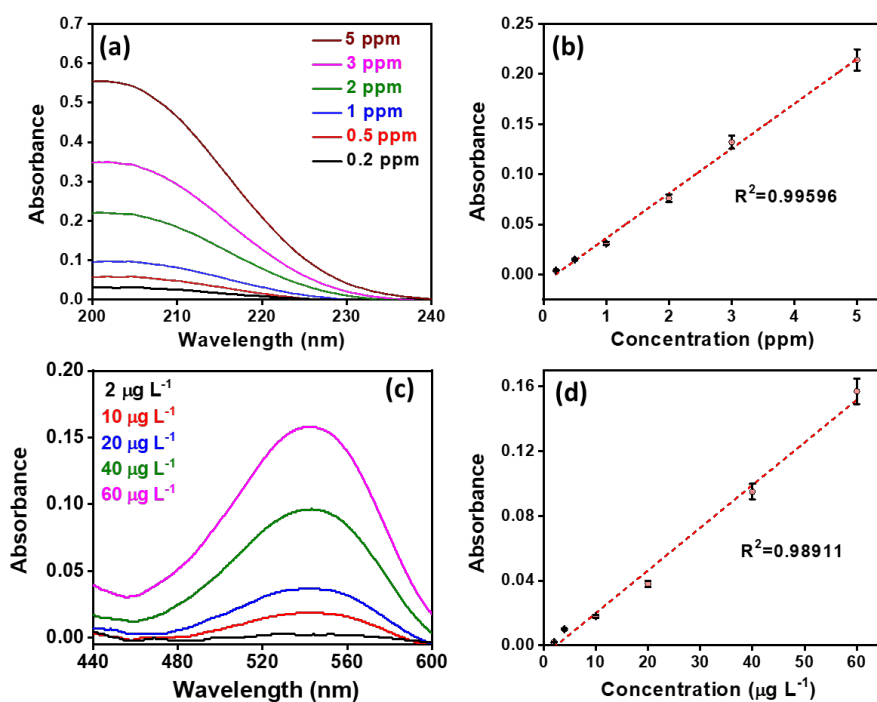


Fig. S11 Absorbance vs. wavelength curves for (a) standard NO_3^- & (c) NO_2^- solutions with different concentrations and (b) & (d) corresponding calibration curves extracted from the same respectively.

S.No.	Gas supply	Conc. of contaminations before purification (ppm)			Conc. of contaminations after purification (ppm)		
		NO/NO ₂	N ₂ O	NH ₄ ⁺	NO/NO ₂	N ₂ O	NH ₄ ⁺
1.	Ar (99.99%, Sigma)	0.6	<0.01	-	-	-	-
2.	¹⁴ N ₂ (99.99% Sigma)	1.1	0.06	0.09	<0.01	<0.01	-
3.	¹⁵ N ₂ (98%, Sigma)	1.2	0.07	0.08	<0.01	<0.01	-

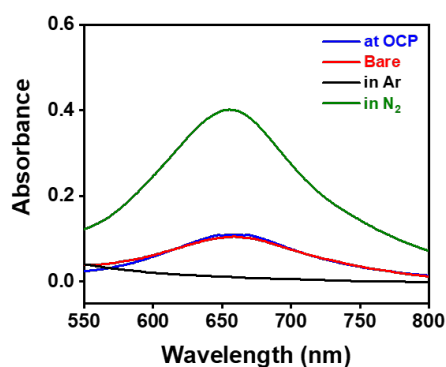


Fig. S12 UV-Vis. absorbance curves obtained after control NRR experiments over bare glassy carbon electrode and $\text{Ag}_2\text{VO}_2\text{PO}_4$ (s) coated glassy carbon electrode in N_2 -saturated, Ar-saturated electrolyte media at -0.2 V and in N_2 saturated conditions at open circuit voltage.

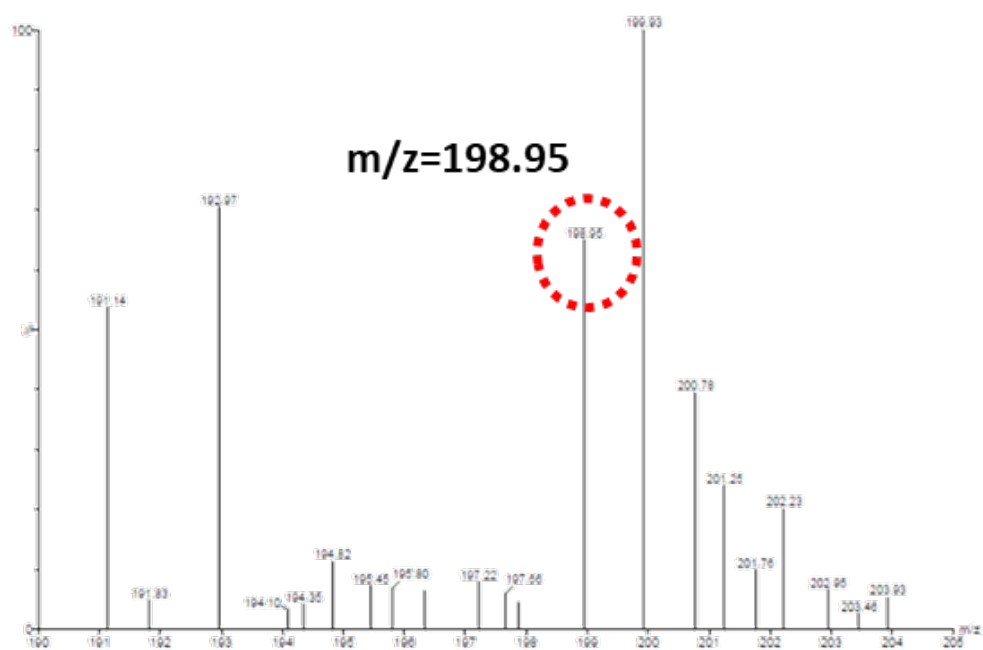
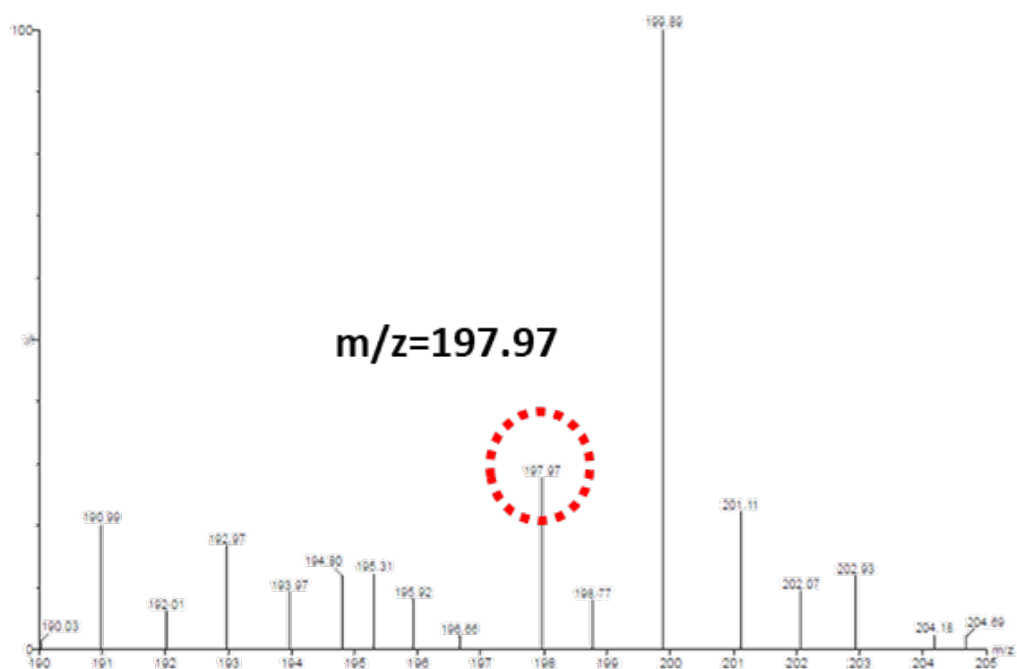


Fig. S13A The mass spectrum for electrolyte samples collected after isotope labelling NRR experiments by $\text{Ag}_2\text{VO}_2\text{PO}_4$ (s) catalyst showing formation of ^{14}N -Indophenol and ^{15}N -indophenol red dye respectively.

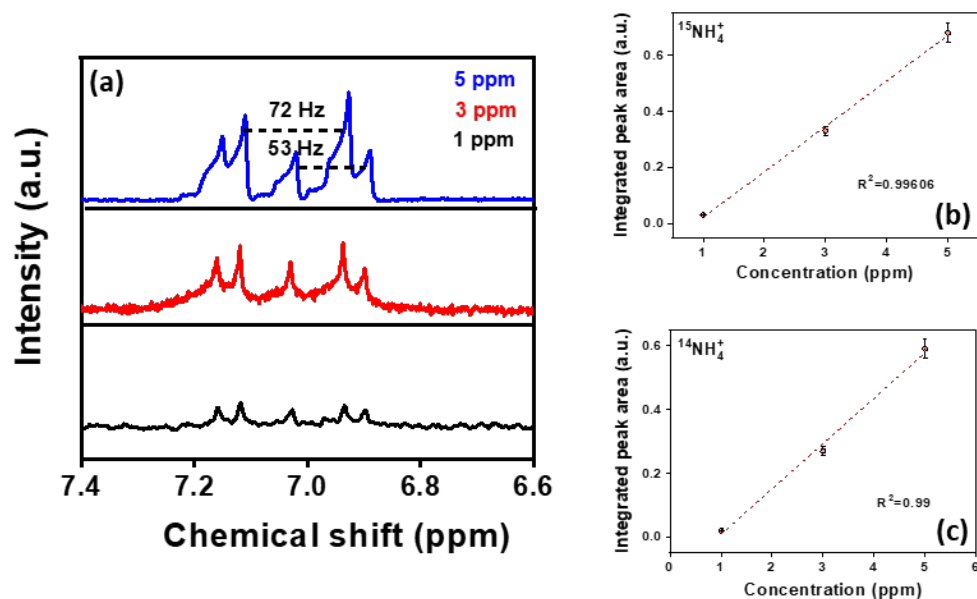


Fig. S13B (a) $^1\text{H-NMR}$ spectrum acquired for standard mixture solutions of $^{14}\text{NH}_4^+$ and $^{15}\text{NH}_4^+$ samples and respective (b-c) concentration vs. integrated peak area plots for quantitative analysis.

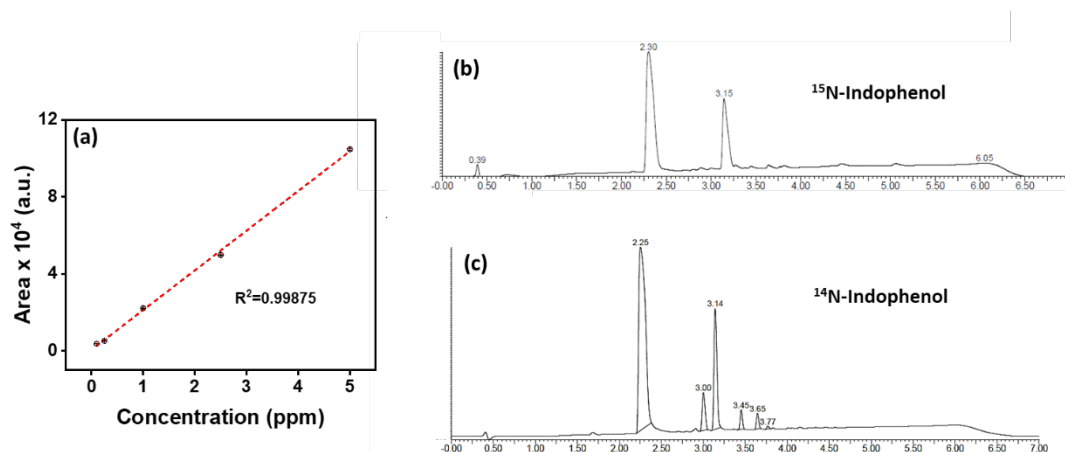


Fig. S13C (a) Concentration vs. integrated peak area plots for quantitative analysis obtained from liquid chromatograms of standard solutions of Indophenol red dye. (b) and (c) Liquid chromatograms obtained for electrolyte sample solutions collected after 2 hours of isotope labelling NRR experiments by $\text{Ag}_2\text{VO}_2\text{PO}_4$ (s) catalyst at -0.2 V (vs. RHE).

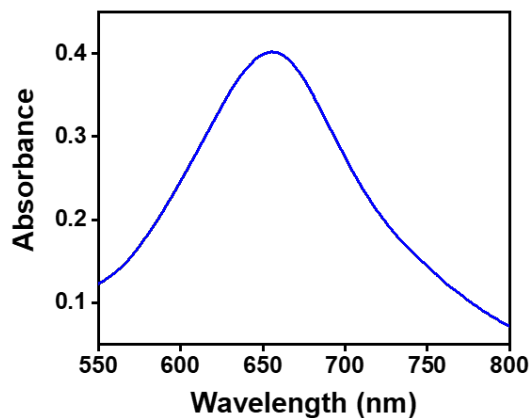


Fig. S13D UV-Vis. absorbance curve obtained after isotope labelling NRR measurement at -0.2 V by $\text{Ag}_2\text{VO}_2\text{PO}_4$ (s) catalyst in $^{15}\text{N}_2$ -saturated 0.1 M KOH solution.

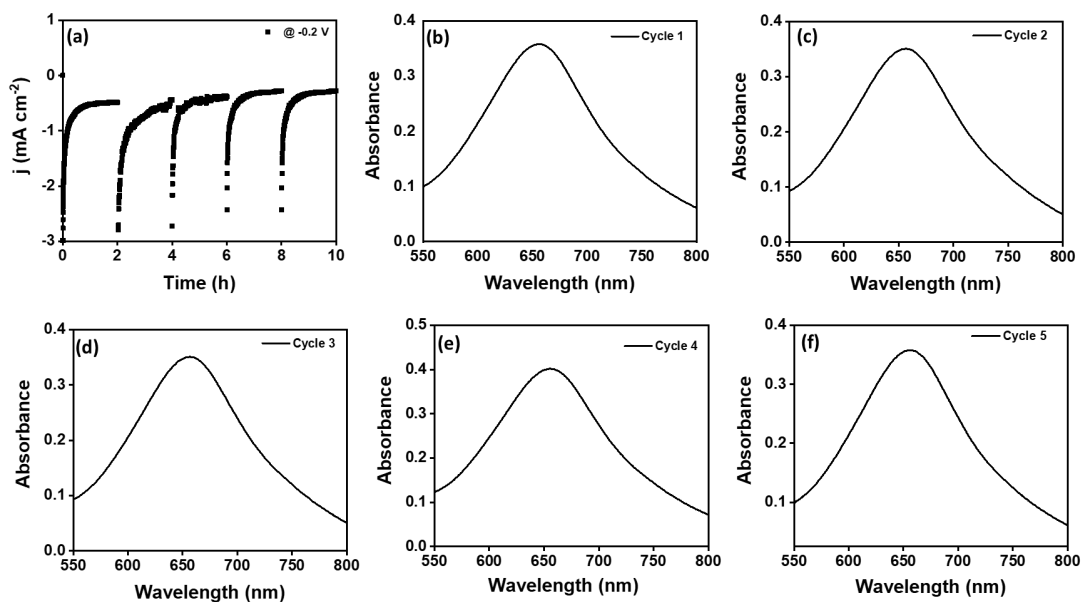


Fig. S14 (a) Chronoamperometry curves for NRR stability tests (5 consecutive cycles) in 0.1 M KOH solution by $\text{Ag}_2\text{VO}_2\text{PO}_4$ (s) catalyst at -0.2 V of applied potential. (b-f) UV-Vis. absorbance curves obtained for electrolyte solutions after every 2 h of NRR stability tests via Indophenol blue method.

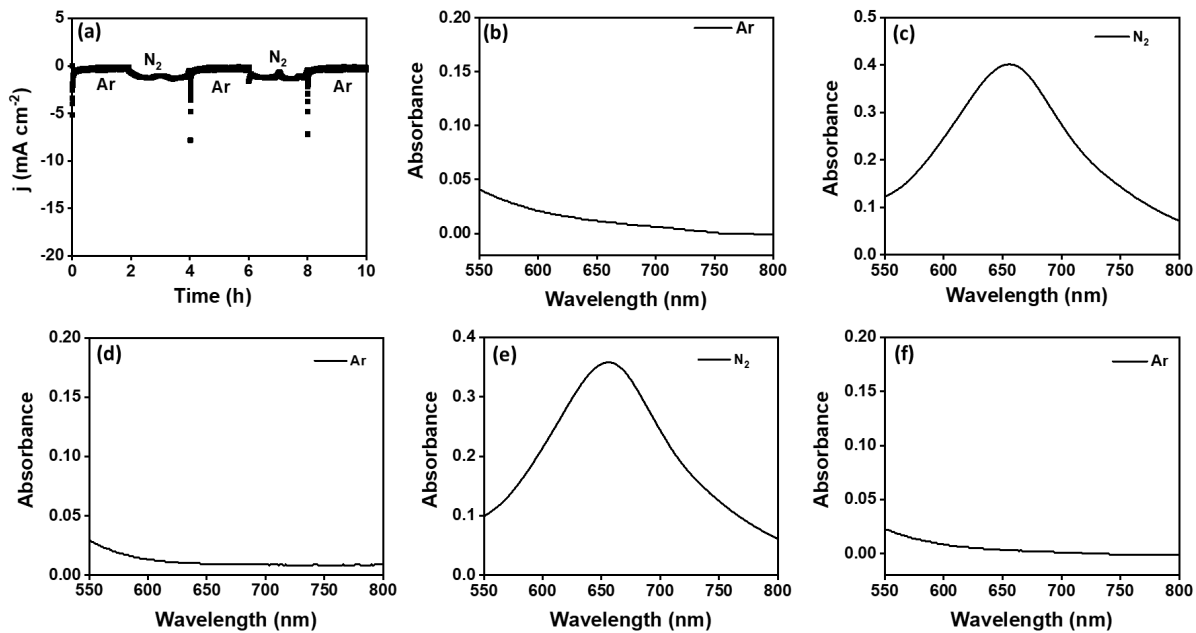


Fig. S15 (a) Switching chronoamperometry curves for $\text{Ag}_2\text{VO}_2\text{PO}_4$ (s) catalyst in different gas-feed environments (Ar and N_2). (b-f) UV-Vis. absorbance curves obtained for electrolyte solutions after every 2 h of NRR stability tests via Indophenol blue method.

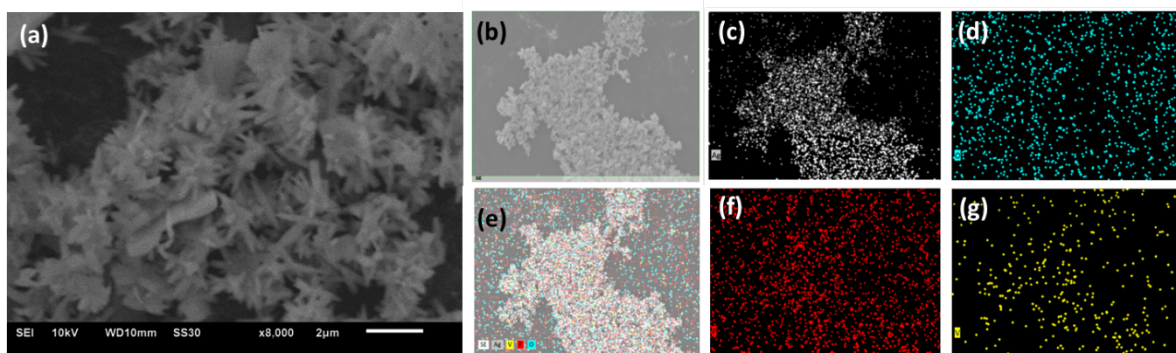


Fig. S16 (a) SEM image, (b-g) EDS dot mapping profiles for individual elements for $\text{Ag}_2\text{VO}_2\text{PO}_4$ (s) catalyst after NRR stability tests.

Catalyst	Electrolyte	R_{NH_3} ($\mu\text{g h}^{-1} \text{mg}^{-1}$)	Pot. vs. RHE	F.E. (%)	References
Ag nanosheets	0.1 M HCl	$4.62 \times 10^{-11} \text{ mol cm}^{-2} \text{ s}^{-1}$	-0.6 V	4.8	⁵ <i>Chem. Commun.</i> , 2018, 54 , 11427-11430.
B-Ag NSs	0.1 M HCl	26.48	-0.5 V	8.86	⁶ <i>Chem. Commun.</i> , 2019, 55 , 14745-14748
Pd-Ag-S PNSs	0.1 M Na ₂ SO ₄	9.73	-0.2 V	18.41	⁷ <i>Nanoscale</i> , 2020, 12 , 13507-13512
Ag NPs-rGO	0.1 M Na ₂ SO ₄	18.86	-0.7 V	3.36	⁸ <i>J. Mater. Sci.</i> , 2020, 55 , 5203-5210
Ag NPs	0.1 M Na ₂ SO ₄	9.23	-0.7 V	2.25	⁸ <i>J. Mater. Sci.</i> , 2020, 55 , 5203-5210
BD/Ag-AF	0.1 M Na ₂ SO ₄	$2.07 \times 10^{-11} \text{ mol cm}^{-2} \text{ s}^{-1}$	-0.6 V	7.36	⁹ <i>Inorg. Chem.</i> , 2018, 57 , 14692-14697
Ag-Au@ZIF	0.2 M LiCF ₃ SO ₃	$1.09 \times 10^{-11} \text{ mol s}^{-1} \text{ cm}^{-2}$	-2.5 V vs. Ag/AgCl	18 ± 4	¹⁰ <i>Sci. Adv.</i> , 2018, 4 , eaar3208
Ag triangular nanoplates	0.5 M K ₂ SO ₄	58.5 mg h ⁻¹ g ⁻¹	-0.25 V	25	¹¹ <i>Chem. Commun.</i> , 2019, 55 , 10705-10708
Single Ag	0.1 M HCl	270.9	-0.6 V	21.9	¹² <i>ACS Nano</i> , 2020
AgNDs	0.1 M Na ₂ SO ₄ (pH=10.5)	600.4 ± 23.0	-0.25 V	10.1 ± 0.7%	¹³ <i>Commun. Chem.</i> , 2021, 4 , 1-11
Ag ₃ Cu BPNs	0.1 M Na ₂ SO ₄	24.59	-0.5 V	13.28	¹⁴ <i>J. Mater. Chem. A</i> , 2019, 7 , 12526-12531
Ag ₃ PO ₄ (2 h)	0.1 M KOH	456.75	0 V	26.66	¹ <i>J. Mater. Chem. A</i> , 2022, 10 , 20616-20625
Ag₂VO₂PO₄ (s)	0.1 M KOH	1.48 mg h⁻¹ mg_{cat.}⁻¹	-0.2 V	37.46	This work

References

- D. Gupta, A. Kafle, S. Kaur, P. Parimita Mohanty, T. Das, S. Chakraborty, R. Ahuja and T. C. Nagaiah, *J. Mater. Chem. A*, 2022, **10**, 20616-20625.
- D. Ekeberg, G. Ogner, M. Fongen, E. J. Joner and T. Wickstrøm, *J. Environ. Monit.*, 2004, **6**, 621-623.
- D. Gupta, A. Kafle, S. Kaur, P. P. Mohanty, T. Das, S. Chakraborty, R. Ahuja and T. C. Nagaiah, *J. Mater. Chem. A*, 2022.
- S. E. Saji, H. Lu, Z. Lu, A. Carroll and Z. Yin, *Small Methods*, 2021, **5**, 2000694.
- H. Huang, L. Xia, X. Shi, A. M. Asiri and X. Sun, *Chem. Commun.*, 2018, **54**, 11427-11430.
- Y. Li, H. Yu, Z. Wang, S. Liu, Y. Xu, X. Li, L. Wang and H. Wang, *Chem. Commun.*, 2019, **55**, 14745-14748.
- H. Wang, S. Liu, H. Zhang, S. Yin, Y. Xu, X. Li, Z. Wang and L. Wang, *Nanoscale*, 2020.
- N. Khaliq, M. A. Rasheed, G. Cha, M. Khan, S. Karim, P. Schmuki and G. Ali, *Sens. Actuators B Chem.*, 2020, **302**, 127200.
- L. Ji, X. Shi, A. M. Asiri, B. Zheng and X. Sun, *Inorg. Chem.*, 2018, **57**, 14692-14697.
- H. K. Lee, C. S. L. Koh, Y. H. Lee, C. Liu, I. Y. Phang, X. Han, C.-K. Tsung and X. Y. Ling, *Sci. Adv.*, 2018, **4**, eaar3208.
- W.-Y. Gao, Y.-C. Hao, X. Su, L.-W. Chen, T.-A. Bu, N. Zhang, Z.-L. Yu, Z. Zhu and A.-X. Yin, *Chem. Commun.*, 2019, **55**, 10705-10708.
- Y. Chen, R. Guo, X. Peng, X. Wang, X. Liu, J. Ren, J. He, L. Zhuo, J. Sun and Y. Liu, *ACS Nano*, 2020.

13. W. Li, K. Li, Y. Ye, S. Zhang, Y. Liu, G. Wang, C. Liang, H. Zhang and H. Zhao, *Commun. Chem.*, 2021, **4**, 1-11.
14. H. Yu, Z. Wang, D. Yang, X. Qian, Y. Xu, X. Li, H. Wang and L. Wang, *J. Mater. Chem. A*, 2019, **7**, 12526-12531.